Lawrence Berkeley National Laboratory

Recent Work

Title

A STUDY OF PRECIPITATION IN INTERSTITIAL ALLOYS: II. A NEW METASTABLE CARBIDE PHASE IN PLATINUM

Permalink

https://escholarship.org/uc/item/5xm2g7tr

Authors

Witccmb, M. J.
Dahmen, U.
Westmacott, K.H.

Publication Date

1982-07-01

� Lawrence Berkeley Laboratory
UNIVERSITY OF CALIFORNIA

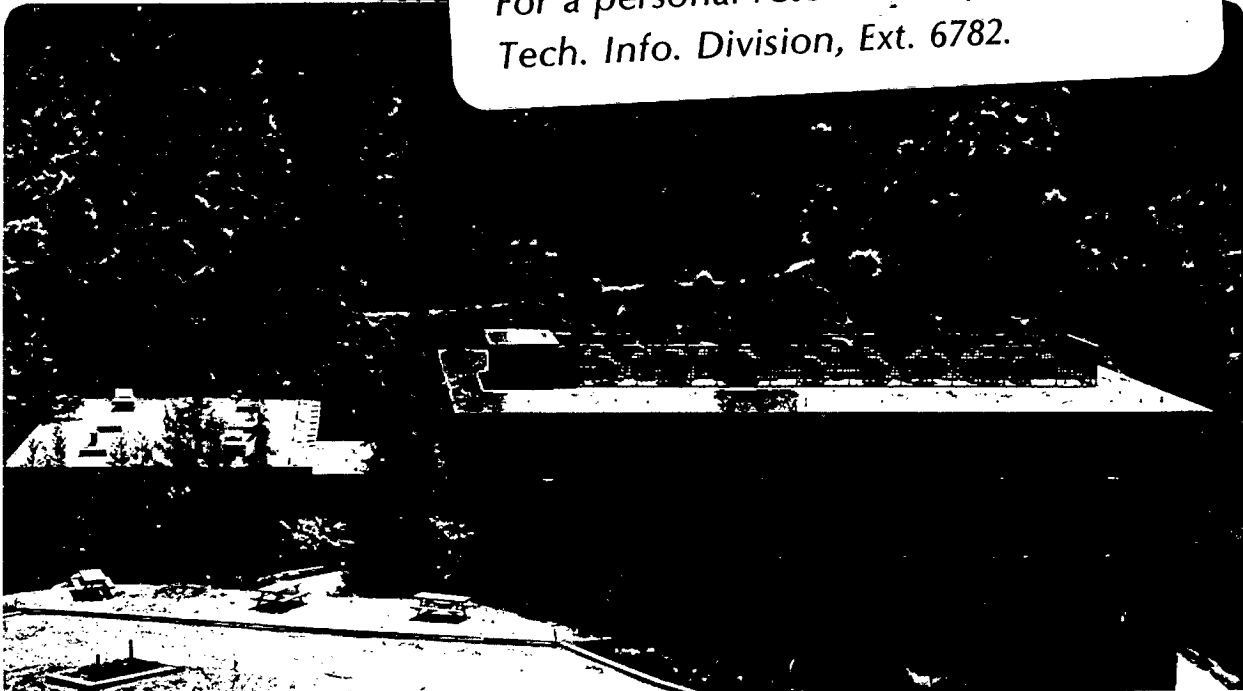## Materials & Molecular Research Division

A STUDY OF PRECIPITATION IN INTERSTITIAL ALLOYS:
II. A NEW METASTABLE CARBIDE PHASE IN PLATINUM

M.J. Witcomb, U. Dahmen, and K.H. Westmacott

July 1982

DISCLAIMER

A STUDY OF PRECIPITATION IN INTERSTITIAL ALLOYS:

II. A NEW METASTABLE CARBIDE PHASE IN PLATINUM

M. J. Witcomb[*], U. Dahmen and K. H. Westmacott

Materials and Molecular Research Division

Lawrence Berkeley Laboratory

University of California

Berkeley, California 94720

[*]Electron Microscopy Unit, University of the Witwatersrand, Johannesburg, S. A.

ABSTRACT

Contrast and convergent beam diffraction studies of precipitates in quenched, aged platinum containing about 800 atomic ppm carbon have identified a body-centered tetragonal structure with a = 0.39nm, c = 0.59nm, c/a = 1.5. An investigation of the microstructure of similarly treated platinum of various purities and of platinum doped with carbon indicates the precipitates to be a metastable carbide of composition at or close to Pt_2C.

INTRODUCTION

According to the data given by Hansen [1], molten platinum and other metals in its groups dissolve substantial amounts of carbon (~1.5w/o) which depresses the melting point. On solidification the solubility is greatly diminished and the excess carbon precipitates as graphite in a eutectic-like matrix. There is a marked disagreement on the solid solubility as attested to by the two orders of magnitude discrepancy in the reported values [2,3]. Both studies agree, however, that the low temperature solubility is vanishingly small, so that even small amounts of retained carbon become supersaturated below ~500°C. No reports have been made of a phase intermediate between the supersaturated solid solution and the equilibrium graphite phase although an electron diffraction study of co-deposited and heated platinum and carbon did reveal superlattice spots indicative of such a phase [4].

Quenching studies on platinum have provided other indirect evidence that carbon or other interstitial impurites are often present in sufficient concentrations to affect properties through perturbation of the vacancy behavior. For example, Mišek [5] has attributed the cyclic changes in resistivity during air and vacuum annealing to changes in the concentration of carbon present in the platinum.

More recent studies of the secondary defect structures formed by direct quenching of platinum into a salt bath at 400°C [6], or quenching to room temperature followed by aging at 400°C [7], have shown that defects often precipitate on {001} planes which is unusual for fcc metals. These defects were best interpreted not solely as faulted vacancy loops, but as the co-precipitation of tightly-bound carbon atom-vacancy complexes [7,8]. The large residual holes associated with vacancy collapse on {001} accommodate the oversized carbon thus reducing the lattice strain associated with their original occupancy of octahedral interstitial sites.

In spite of the fact that in these alloys the Pt-vacancy system is perturbed by only a small interstitial carbon concentration ($\sim 10^{-4}$), microstructures of striking complexity develop during post-quench aging treatments. Nevertheless, a logical sequence of development has been established.

The present paper gives (i) the evidence used to infer that the observed defect structures represent the nucleation and growth of an intermediate carbide phase from supersaturated solid solution, and (ii) a convergent beam diffraction analysis which identifies this new phase as body-centered tetragonal with a stoichiometric composition of Pt_2C.

In the paper which follows this, a theoretical framework for describing possible precipitate growth processes is developed and applied to the Pt-C case (III). A further paper (IV) discusses the entire precipitation sequence and the interplay between vacancies, dislocations, and precipitate development.

EXPERIMENTAL METHODS

Several grades of platinum obtained from different sources were used in the experiments. To maintain the original impurity content and ensure reproducibility, all the quenching was performed in a high vacuum system pumped and baked to a base pressure in the 10^{-7} Pa range. This clean quenching environment was obtained, however, at the expense of a relatively slow quench rate ($1000^\circ Cs^{-1}$). During heating to the quenching temperature (usually the melting point), the pressure increased to no more than 4×10^{-6} Pa. Subsequently, the samples were aged in air or at 10^{-6} Pa. Electron transparent foils were prepared in an electropolishing bath of equal volumes of nitric, phosphoric and sulphuric acids operated at room temperature and ~ 3 volts AC [9]. The foils were studied in various 100kV, 125kV and high voltage electron microscopes.

RESULTS

The Origin of the Precipitate Structures. Two difficulties arise in directly proving the presence of carbon and estimating its concentration in platinum. The first is the uncertainty in placing limits on the amounts that could be dissolved and precipitated (see Introduction), while the second is the problem of obtaining a reliable quantitative determination of impurity levels close to detection limits. Consequently, indirect methods were used to deduce that the observed microstructures resulted solely from carbon precipitation.

Most of the experiments were performed on a relatively impure grade of platinum containing $\sim$ 0.5 a/o substitutional impurities (principally Rh, Pd, and Ir) and an estimated carbon concentration of $\leq 8 \times 10^{-4}$. The microstructures observed in this material after quenching and quench-aging at 400°C are shown in Figs. 1 and 2, respectively. The precipitates are visible mainly through displacement fringe contrast. The displacement vector of the precipitates was found to be close to $\frac{a}{3}$ <001> in the as-quenched condition and $\frac{a}{2}$ <001> after aging at 400°C (see paper IV). Precipitate identification is thus straightforward since both types of precipitate will show displacement fringes in an image obtained with a <111> diffraction vector (Figs. 1b, 2b); the $\frac{a}{2}$ <001> precipitate fringes disappear when using a <220> diffraction vector (Fig. 2a); perfect-loops will never show fringes.

Similarly treated foils of a very well characterized platinum obtained from the National Bureau of Standards were also studied. Spectrographic analysis revealed that the total atomic concentration of substitutional impurities in this material was only $\sim 5 \times 10^{-6}$. No information is available as to the carbon concentration. However, the indications are that it is similar to the impure Pt since after quench-aging (Fig. 3) the structures were indistinguishable from those seen in Fig. 2.

A third grade of Pt obtained from Engelhard Industries fortuitously proved to

be purer in terms of <u>interstitial</u> impurities. In the as-quenched condition, this material contained perfect prismatic dislocation loops rather than plate precipitates (see Fig. 4). Despite the small size of the loops, the difference in diffraction contrast from similarly sized precipitates in Fig. 1 is evident. This difference is even more apparent after aging at 515°C. While Fig. 5 reveals that the loops have annealed and coarsened, it is clear that no precipitates are present when a comparison is made with the corresponding microstructures of the two grades of material containing carbon impurities (Figs. 2 and 3). Finally, Fig. 6 illustrates the microstructures found in the Engelhard material after it had been deliberately doped with carbon by heating in a carburizing atmosphere of acetylene prior to quenching and aging. A full contrast and convergent beam diffraction analysis provided unambiguous proof that the defects present after this treatment were identical to those found in the impure and NBS grades of platinum. (Compare Fig. 6 with Figs. 2 and 3.).

Since the first two experiments show that changing the substitutional impurity level by a factor of 10^3 had no effect, the microstructures must arise from the precipitation of an interstitial impurity. The second two experiments show this interstitial impurity to be carbon.

Two other possible impurities, oxygen and hydrogen, may be dismissed on the following grounds: (i) the measured solid solubilities of both oxygen and hydrogen are two to three orders of magnitude lower than carbon [10]; (ii) the high vacuum techniques used should exclude these impurities and reduce their initial concentrations; and (iii) earlier [7] and present experiments have shown that quenching from an oxygen-containing atmosphere leads to replacement of the precipitate structure by a void structure; and (iv) the structures were found to be independent of the electropolishing solution used [6], which eliminates the possibility of hydrogen contamination.

Thus it may be concluded that the observed microstructures develop when small amounts ($10^{-3} - 10^{-4}$) of interstitially dissolved carbon precipitate from solid solution during aging following a rapid quench.

The Nature of the Intermediate Precipitates. During post-quench annealing of foils at temperatures in the range 400-530°C, the precipitates characterized by $\frac{a}{2}$ <00l> displacement vectors increased in average size and decreased in density. At this point, the capability of the Philips EM400 to produce a fine electron probe was used to obtain convergent beam diffraction patterns (in TEM mode operation) from individual precipitate plates. The high angle tilting stage and excellent vacuum conditions permitted the patterns from up to ten low order zones to be recorded from the same precipitate. Because the plates are only a few monolayers thick, very long exposure and developing times were necessary [11].

The series of pictures presented in Fig. 7 shows the patterns obtained with the electron beam oriented along three of the matrix zone axes recorded. The extra spots, though faint, are readily discernible. Patterns taken from the matrix adjacent to the precipitate showed only spots characteristic of the pure Pt fcc structure. The reciprocal lattice model for the precipitate was reconstructed from the information contained in the reciprocal lattice sections and is illustrated in Fig. 8a. It is evident that the precipitate structure is body-centered-tetragonal with a c/a ratio of 3/2. Furthermore, the positions of the superlattice reflections are consistent with platinum atoms at (0 0 0), (0 0 $\frac{1}{2}$), ($\frac{1}{2}$ $\frac{1}{2}$ 0) and ($\frac{1}{2}$ $\frac{1}{2}$ $\frac{1}{2}$) and carbon atoms at ($\frac{1}{2}$ 0 $\frac{1}{4}$) and (1 $\frac{1}{2}$ $\frac{3}{4}$) corresponding to a structure factor equation:

$$F_{hkl} = [f_{Pt}(1 + e^{\pi i \ell}) + f_C e^{\pi i(h+ \ell/2)}][1 + e^{\pi i(h+k+\ell)}] \quad .$$

If it is assumed that all the carbon sites are filled, the carbide composition is Pt_2C. A diagram of the unit cell of this structure is given in Fig. 8b.

DISCUSSION

Although the present observations constitute the first evidence for intermediate phase formation in Pt-C, it is not altogether surprising since a carbide phase with an orthorhombic structure has been reported in Ni [12]. Both metals are in the same group of the periodic table and had been thought to form only graphite structures.

It is seen from Fig. 8 that the Pt_2C structure is anti-isomorphous with calcium fluorite. Most ionic compounds in this structural class form from atoms with large differences in electronegativity. Pt_2C is apparently an exception if the Pauling values for electronegativity are used (Pt 2.2, C 2.5), nevertheless its stability can be attributed to the formation of stable octets of valency electrons. It may constitute an intermediate phase which provides a more energetically favorable path to graphitization.

The Pt_2C is somewhat analogous to the metastable ε carbide phase that forms in ferrous alloys in that both precipitate as platelets on the {001} matrix planes, and are transition phases in a sequence ending in graphite formation. However, the 50% volume misfit of the Pt_2C in platinum is very much greater, and it will therefore be more difficult to nucleate.

Close analogies also exist with the formation of θ' in Al-Cu and η in Al-Au. Both of these phases precipitate as plates on the {001} matrix planes and have tetragonal symmetry with crystal axes parallel to those of the matrix. There is a significant difference, however, in that both θ' Al_2Cu and η Al_2Au are substitutional phases which are undersize relative to the Al matrix whereas the Pt_2C is interstitial and oversize in the Pt. Nevertheless, there is a close connection between the formation mechanisms of these phases and this aspect is discussed further in the two companion papers.

CONCLUSIONS

1. During aging following a rapid quench from high temperatures, a precipitation reaction occurs in platinum containing small amounts of carbon.

2. A new metastable carbide phase with a composition at or close to Pt_2C has been identified. Its crystal structure is body-centered tetragonal with a c/a ratio of 3/2.

ACKNOWLEDGEMENTS

REFERENCES

1. M. Hansen, <u>Constitution of Binary Alloys</u>, McGraw-Hill, New York (1958), p. 377.

2. R. H. Siller, W. A. Oates and R. B. McLellan, J. Less Common Metals $\underline{16}$, 71 (1968).

3. G. L. Selman, P. J. Ellison and A. S. Darling, Platinum Met. Rev. $\underline{14}$, 14 (1970).

4. H. König, Naturwissenschaften $\underline{38}$, 154 (1951).

5. K. Misek, Czech. J. Phys. $\underline{B17}$, 647 (1967).

6. K. H. Westmacott, J. Phys. F: Met. Phys. $\underline{3}$, L217 (1973).

7. K. H. Westmacott, Cryst. Latt. Defects $\underline{6}$, 203 (1976).

8. K. H. Westmacott and M. I. Perez, J. Nucl. Mat. $\underline{83}$, 231 (1979).

9. J. Tousek, Praktische Metall. $\underline{7}$, 202 (1970).

10. <u>Gase und Kohlenstoff in Metallen</u>, Springer, Berlin (1976), p. 650.

11. M. J. Witcomb, Ultramicroscopy $\underline{7}$, 343 (1982).

12. M. Nemoto, K. Onisawa and H. Suto, Trans. Jap. Inst. Met. $\underline{18}$, 331 (1977).

Figure Captions

Fig. 1. Precipitate plates on {001} planes in impure Pt quenched from near the melting point and imaged with a <220> diffraction vector in (a), and a <111> diffraction vector in (b). Displacement fringes are observed in both g = <111> and <220>, whereas dislocation contrast is observed only for one of the precipitate variants in <220>.

Fig. 2. Microstructure in same material as Fig. 1 after a post-quench aging treatment of 24h at 400°C. Under the same diffracting conditions, fringes were now observed with g = <111> but not with g = <220>. Micrographs by M. Perez.

Fig. 3. {001} precipitates in "super-purity" NBS Pt quenched from the melting point and subsequently aged for 24h at 400°C. A comparison with Fig. 2 shows that the large precipitate plates (e.g. at A) in each material exhibit identical contrast behavior. The smaller precipitates (B) are those characterized in the as-quenched state in Fig. 1. Micrographs by M. Perez.

Fig. 4. Dislocation loop structure in as-quenched foil of Engelhard-supplied Pt. (a) shows the g = <220> image and (b) the <111> image. Note the absence of displacement contrast and the strong dislocation contrast in both reflections.

Fig. 5. Same material as Fig. 4 after a post-quench age for 1h at 515°C showing low density of large perfect prismatic dislocation loops. The image characteristics were identical to those observed for the as-quenched defects in Fig. 4.

Fig. 6. Precipitate structures in the Engelhard Pt after it had been carburized by heating in acetylene, then quenched and aged 1h at 500°C. A comparison with Figs. 2 and 3 shows the contrast behavior to be the same.

Fig. 7. Typical examples of the convergent-beam diffraction patterns obtained from individual precipitates in the quenched-aged impure Pt. The electron beam was directed along the <001> zone axis in (a), the <112> in (b), and the <123> in (c). The extra reflections and streaks associated with the precipitate structure are readily apparent.

Fig. 8. (a) shows the reciprocal lattice model for the precipitate constructed from extra spots observed in the diffraction patterns; (b) diagram of a unit cell of the precipitate structure derived from the solution of the structure factor equation emphasizing the distorted tetrahedral coordination of the carbon around the Pt and the distorted octahedral distribution of Pt around the carbon.

g $\bar{2}\bar{2}0$

0.2 μm

Fig. 1

g $\bar{1}1\bar{1}$

XBB 827-5939

g $20\bar{2}$

Fig. 2

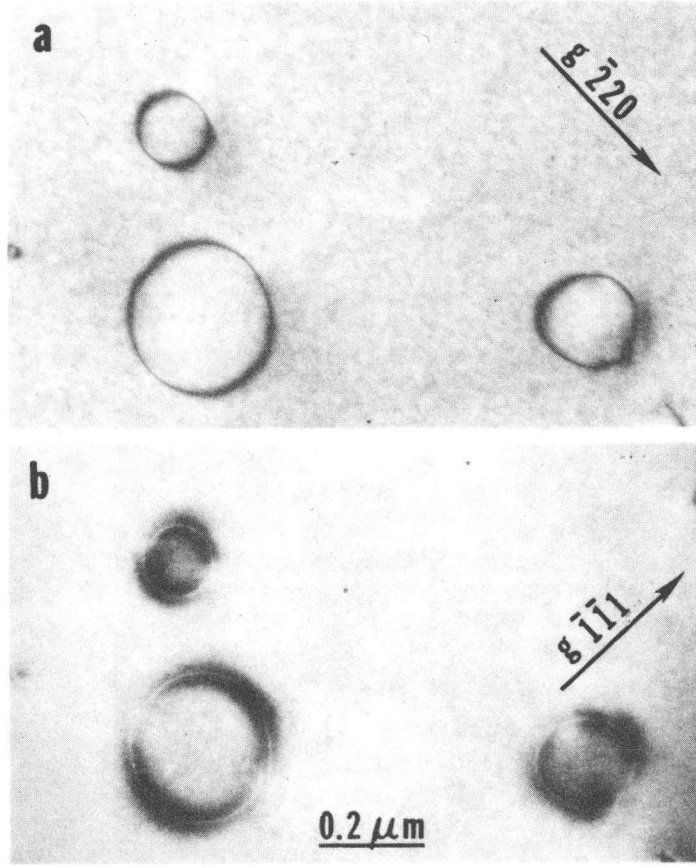g $11\bar{1}$

0.2 μm
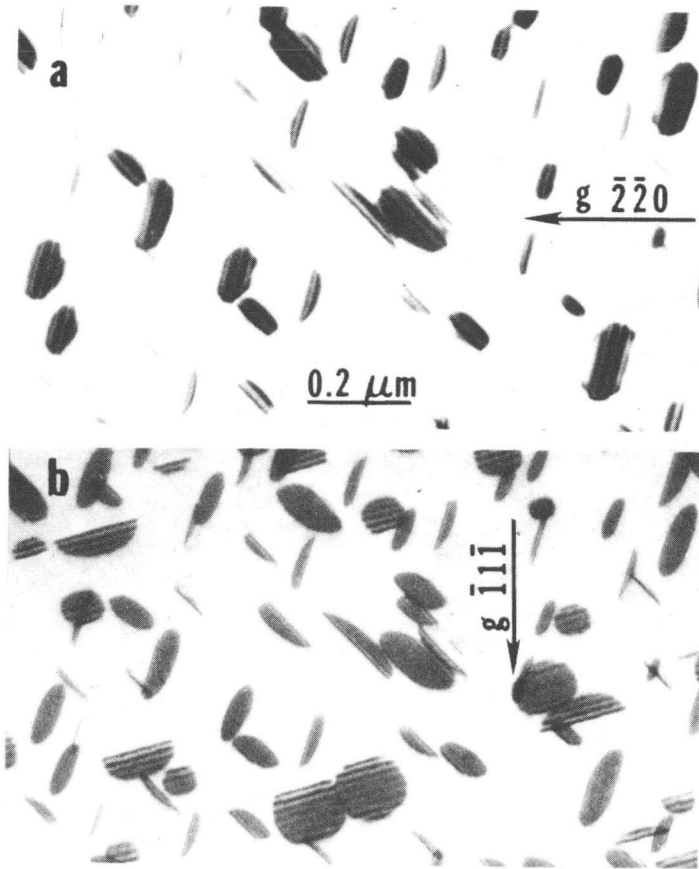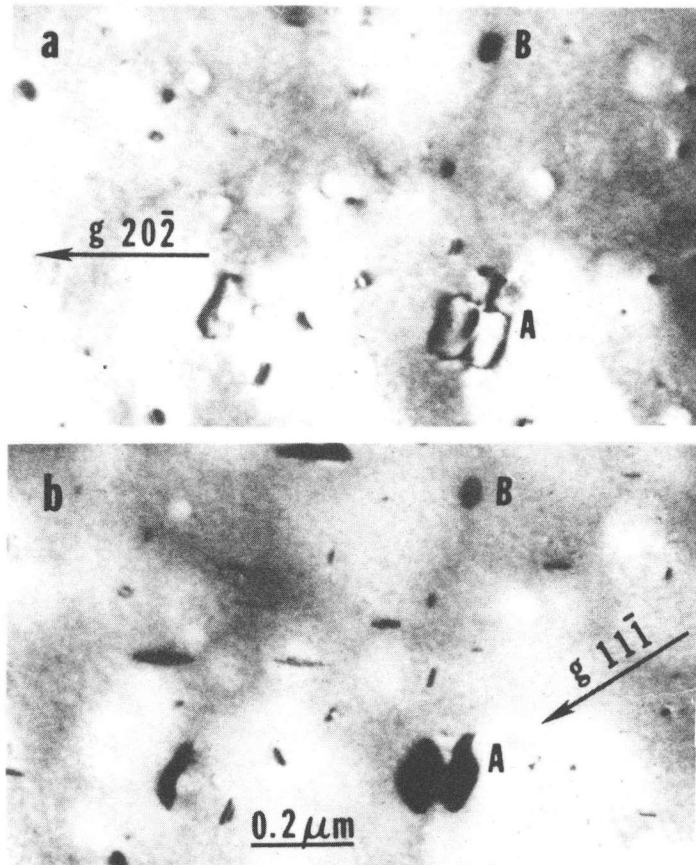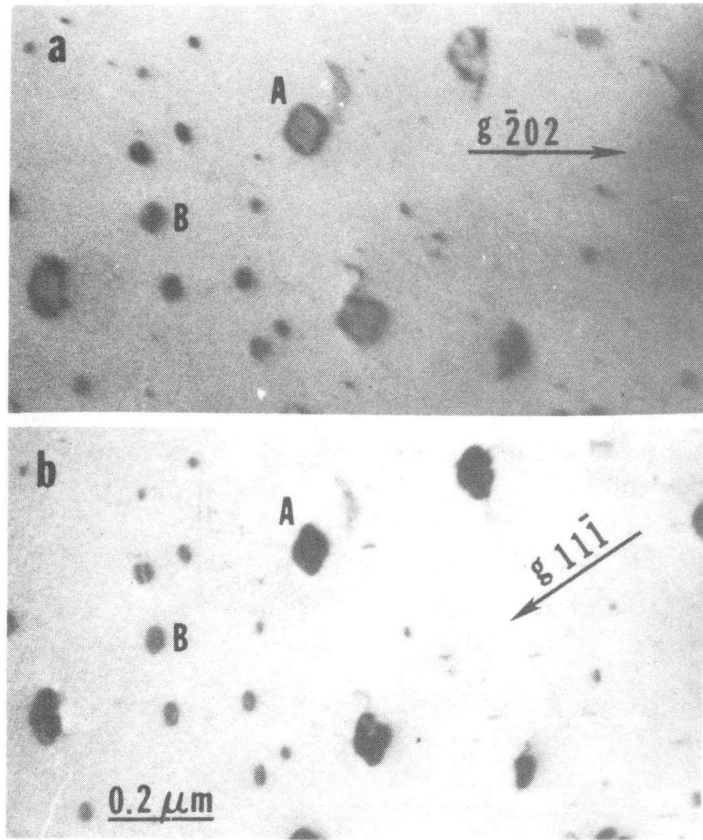
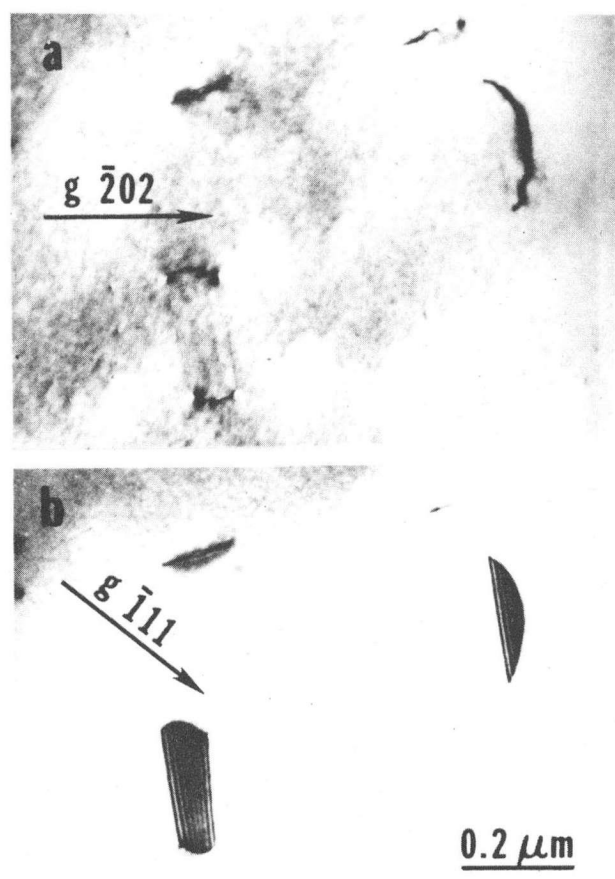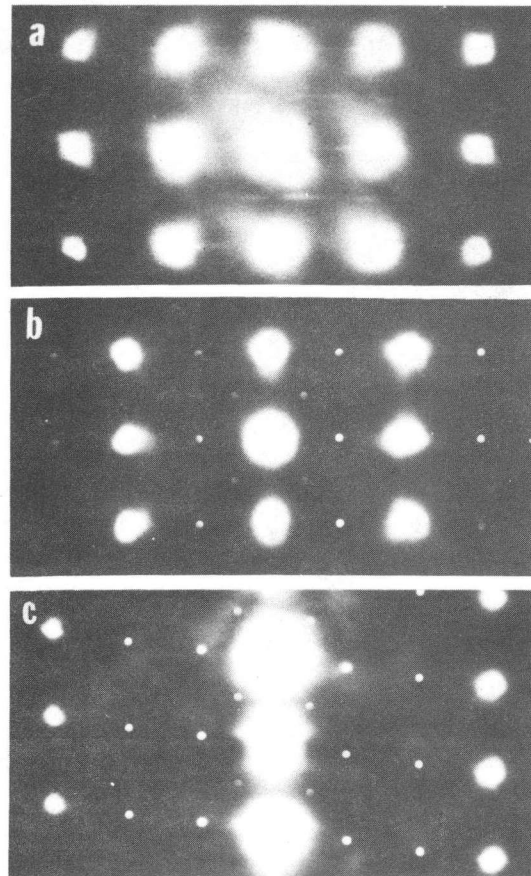XBB 827-5940

Fig. 3

XBB 827-5941
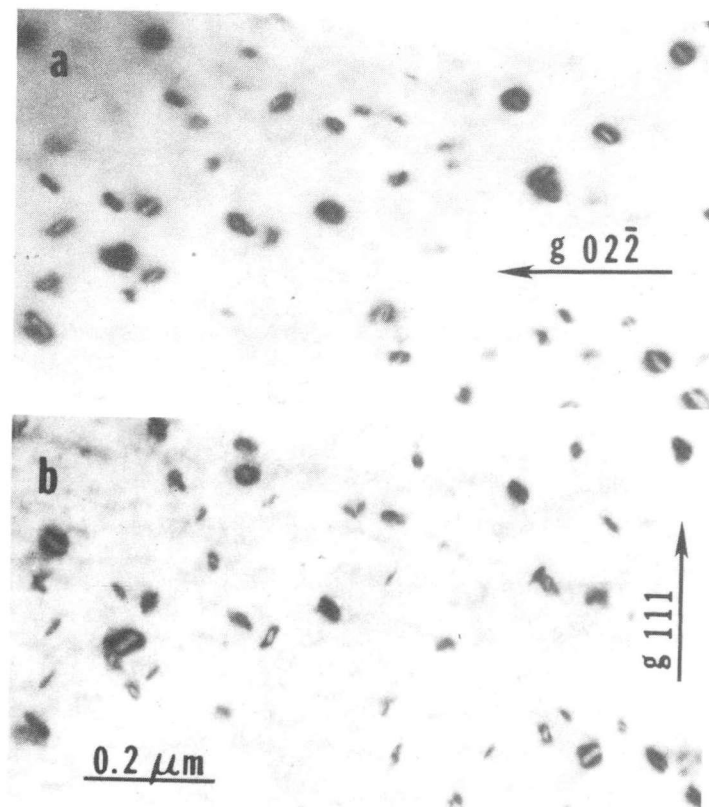
Fig. 4

XBB 827-5942

Fig. 5

XBB 827-5943

Fig. 6

XBB 827-5944

XBB 827-5935

Fig. 7

TECHNICAL INFORMATION DEPARTMENT
LAWRENCE BERKELEY LABORATORY
UNIVERSITY OF CALIFORNIA
BERKELEY, CALIFORNIA 94720